

OPTICAL OBSERVATIONS OF 22 VIOLENTLY VARIABLE EXTRAGALACTIC SOURCES:1968-1986

JAMES R. WEBB, ALEX G. SMITH, ROBERT J. LEACOCK, GREGORY L. FITZGIBBONS, PAUL P. GOMBOLA,
AND DAVID W. SHEPHERD

Rosemary Hill Observatory, Department of Astronomy, University of Florida, Gainesville, Florida 32611
Received 2 July 1987; revised 27 October 1987

ABSTRACT

Broadband photographic observations of 22 optically violent variable (OVV) active galactic nuclei are presented. Over 3100 observations made between 1968 and 1986 at Rosemary Hill Observatory are tabulated and displayed graphically. The majority of the observations were made in either the Johnson *B* system or the international photographic (PG) system. Multicolor data are presented for a few objects. Descriptions of the light curves include the assignment of each OVV to an arbitrary variability subclass. The light curves, some extending over 18 yr, are analyzed for linear trends and underlying structure using linear regression and unequal-interval Fourier transform techniques. The results of the analysis for each of the 22 objects are given and models of the light variations of 3C 120, 3C 345, and 3C 446 are presented. The models of these light curves show underlying structure with rapid variations superimposed. The timescales seen in the light curves of 3C 120, 3C 345, and 3C 446 are compared with characteristic timescales found in massive-accretion-disk models. The timescales most likely to be responsible for the optical behavior are either the viscous or the thermal timescales.

I. INTRODUCTION

Variability continues to be a major stumbling block in understanding the nature of quasars and other AGNs. Radio emission and the broad, redshifted emission lines were the first indications that these objects were different from any previously known objects. It was optical variability that set severe size limitations on the emission regions and revealed the true ultracompact nature of quasars. Optical variability, with its diverse morphological characteristics and seemingly stochastic nature, is still a problem with which no current model can adequately deal. It is critical to investigate the optical-variability problem; long-term monitoring is a necessary part of this investigation.

The monitoring program carried out at the University of Florida's Rosemary Hill Observatory (RHO) has been in continuous operation since 1968. Photographic observations are made of over 200 quasars, BL Lacertids, and active galaxies. Previous summaries of the data were published by McGimsey *et al.* (1975), Scott *et al.* (1976), Pollock *et al.* (1979), and Pica *et al.* (1980a), hereafter referred to as papers I-IV, respectively.

Two objects, 1156 + 295 and 0215 + 01, have been added to the OVV list in Paper III because of recent attention given them in the literature. Some data reported here have been rereduced since Paper III in light of new comparison sequences (0235 + 164) and improved reduction methods (3C 120). While most of the pre-1979 data remained unchanged, some individual observations were rereduced, and observations made within a 1 hr period were averaged (Paper III lists each exposure separately). This averaging not only makes the tables more tractable, but also yields less cluttered light curves.

II. DATA REDUCTION

Data acquisition and reduction procedures were reported in detail in Paper III, so here we give only a brief summary. Most exposures were made at the $f/4$ Newtonian focus of the 76 cm reflector, but at times a few of the brighter OVVs were photographed at the $f/10.5$ Cassegrain focus of the 46 cm reflector. Tests revealed no significant differences between results from the two instruments. Photographic emulsions

used in the monitoring program are all hypersensitized, and they are exposed in an atmosphere of dry nitrogen to avoid sensitivity changes due to the humid Florida air. The filter/plate combinations for each color system, as well as the hypersensitization techniques for each emulsion, are listed in Table I. Column 1 designates the color systems, in which the *U*, *B*, and *V* systems are equivalent to the standard Johnson *UBV* system. The PG system is the international photographic system, and *I* is on the Kron system. Columns 2 and 3 indicate the filters and emulsions used to obtain each of the color systems, and column 4 lists the hypersensitization technique for each emulsion. Column 5 gives the references to the hypersensitization techniques of column 4. All exposures were developed at 20° C using either MWP-2 (Difley 1968) or Kodak D-19 developers.

The plates were reduced using a Cuffey Variable-Iris Astrophotometer for image measurement and a Commodore PET 2001 microcomputer for magnitude determination. The reduction programs fit a parabolic curve to the comparison-star iris readings and magnitudes. The error quoted in this paper is the rms scatter of the comparison stars around the calibration curve, which we use as a measure of plate quality (Penston and Cannon 1970). Internal comparison of observations of the same object made in rapid succession suggests that the rms is a conservative estimate of the error; i.e., it tends to overestimate the error in the QSO magnitude. This formal error does not include systematic zero-point errors due to errors in the calibration sequence; however, our experience in combining our data with photoelectric observations indicates that significant zero-point errors are rare.

In two cases, 3C 120 and 3C 371, a fixed iris was used to measure the image to minimize effects of the nebulosity surrounding the nuclei. In such cases, the exposure is also reduced to an empirically determined minimum to suppress nebulosity. Comparison sequences for the 22 fields were obtained either through the literature (photoelectric determination of at least eight stars within 0.3° of the object) when available, or by photographic transfer from a nearby calibrated region. A more detailed account of the calibration procedures is given in Paper III.

All data in this paper have been reviewed, and some earlier data have been rereduced since Paper III. We decided to

TABLE I. Filter/plate combinations.

COLOR	FILTER	EMULSION	TREATMENT	REFERENCE
PG	NO FILTER	KODAK 103A-O	NITROGEN BAKED HYDROGEN SOAKED	SCOTT AND SMITH, 1976.
PG	NO FILTER	KODAK IIIA-J	FORMING GAS	SCOTT ET AL., 1977.
U	UG-2	103A-O	NITROGEN BAKED HYDROGEN SOAKED	SCOTT AND SMITH, 1976.
B	GG-385	103A-O	NITROGEN BAKED HYDROGEN SOAKED	SCOTT AND SMITH, 1976.
V	GG-495	IIA-D	NITROGEN BAKED	SCHOENING, 1977.
V	GG-495	103A-D	HYDROGEN SOAKED	
I	I-N	RG-695	FORMING GAS BAKED	SCOTT ET AL., 1977.

republish the pre-1979 data here with the additional 7 yr of data for completeness and to make the data more accessible, along with overall light curves. In some instances, as many as 12 exposures were made within 1 hr. Instead of republishing each exposure separately, we averaged all exposures made within a 1 hr period to reduce the volume of data in the tables and minimize clutter in the light curves. The averaging formula weights each exposure by the inverse square of its rms error and calculates the mean magnitude and the combined rms error.

Averaging resulted in a very few cases in reducing the rms errors below 0.01 mag. Since OVVs have been observed to fluctuate 0.01 mag within 1 hr periods (Angione 1971; Kinman 1978; Racine 1970; and Wills *et al.* 1983), we rounded errors smaller than 0.01 up to 0.01. Only three sets of observations of BL Lac were actually affected by this convention.

Errors induced by airmass effects and/or plate inhomogeneities were discussed extensively in earlier publications of the Florida group. Some of this work is reviewed in Pica *et al.* (1987). In that work, each of the 12 to 15 comparison stars in six QSO fields was treated as an unknown; in no case did either the light curve or the chi-square analysis suggest variability of a comparison star, in contrast to the results obtained for the QSOs. Much earlier, Hackney (1972) made both theoretical and experimental studies of the airmass problem. His results indicated that any airmass errors would be hidden in the normal scatter of the photographic data unless observations were made at improbably large zenith distances.

III. OBSERVATIONS

The 22 OVVs are listed in Table II, along with their 1950 coordinates and monitoring information. Columns 1 through 3 list the common name and the right ascension and declination. Column 4 gives the total number of observations for each object, while column 5 indicates the dates between which these observations were made. Column 6 describes the appearance of the light curves in terms of variability subclasses, and column 7 indicates the color system in which each OVV was observed. Column 8 lists the average rms error for each object.

Variability subclasses (Dent *et al.* 1974) are chosen on the basis of the appearance of the optical light curves (see Paper I). An object is assigned to subclass I if its light curve shows

rapid flickering without significant long-term trends. Conversely, subclass II shows slow, long-term changes of larger amplitude than any short-term variations. Subclass III is characterized by comparable amplitudes of short- and long-term variations. Finally, subclass IV is defined as episodic, usually showing large-amplitude outbursts with long intervening inactive periods. Only two subclass changes from Paper III were necessary when the objects were reclassified using the additional 7 yr of data. These subclass assignments are presently subjective, and no connection between the subclasses and the underlying physics is known.

The observations are presented in Table III. The first column gives the universal date of the observation, while column 2 lists the Julian date (JD - 2,400,000). Column 3 reports the magnitude (the color system is indicated in the heading of each section), column 4 gives the rms error, and column 5 indicates the number of exposures averaged. If no entry is made in column 5, the magnitude and rms represent a single exposure. The observations are also presented graphically in Fig. 1. The light curves are arranged in order of right ascension, except for those of OJ 287 and BL Lac, which were placed out of order to conserve space. The apparent magnitude is plotted versus date for each object. Where a substantial amount of *U*, *V*, or *I* data are available, it is also plotted for direct comparison. The error bar in the upper left-hand corner of each plot represents an error of ± 0.1 mag.

In the remainder of this section each OVV will be discussed individually, concentrating on its activity since 1979. The reader is referred to Paper III for references to comparison sequences, finder charts, and pre-1979 discussions. The references for objects not included in Paper III are discussed below. Comparison sequences calibrated at RHO are available by request from the authors.

0215 + 01. The BL Lac object 0215 + 01 was identified by Bolton and Wall (1970), and shown to have no emission lines in its spectrum by Wills and Lynds (1978). We added this OVV to our program in 1981 and detected optical variability over a 3.5 mag range. The comparison field calibration was done by transfer from Selected Area 94 on 24 November 1981. Blades *et al.* (1982) mention that this object had a range of 4 mag. Our brightest measured *B* magnitude was 14.5 on 20 October 1984, while the faintest was 18.0 on 11 August 1983. In late 1985, 0215 + 01 was again very faint, but by the end of 1986 it was once more brightening.

TABLE II. Source monitoring data.

SOURCE NAME	RIGHT ASCENSION (HMS)	DECLINATION (DMS)	# OBS.	MONITORING PERIOD	SUBCLASS	COLOR SYSTEM	AVERAGE RMS
0215+01	02 15 13.5	+01 30 54	48	9/25/81-11/4/85	III	B	0.15
0235+16	02 35 52.6	+16 24 05	121	12/29/75-2/1/86	I	B	0.17
OE 110	03 06 20.7	+10 17 56	62	1/2/75-1/20/85	III	B	0.13
0420-01	04 20 43.1	-01 27 32	126	12/4/69-1/31/86	III*	PG	0.22
3C 120	04 30 31.6	+05 14 53	127	10/16/71-2/3/86	II	B	0.11
NRAO 190	04 40 04.7	-00 23 16	84	12/8/69-3/7/86	III	PG	0.16
0735+17	07 35 14.3	+17 49 12	153	4/19/74-3/31/86	III	B,U,V,I	0.13
OJ 287	08 51 57.5	+20 18 00	279	12/15/71-4/1/86	II	B,U,V,I	0.12
0906+01	09 06 35.7	01 33 53	195	3/20/69-3/31/86	I	B	0.10
1156+295	11 56 58.1	+29 31 24	145	5/9/80-4/12/86	I	B	0.15
ON 231	12 19 01.0	+28 30 36	117	2/22/72-4/3/86	I	B	0.16
1308+32	13 08 08.2	+32 36 54	105	4/22/76-2/13/86	III	B	0.18
1514-24	15 14 45.0	-24 11-20	101	2/20/72-4/14/86	I	B	0.16
NRAO 512	16 38 49.0	+39 53 00	196	5/7/70-4/10/86	III	PG	0.15
3C 345	16 41 17.7	+39 54 11	212	6/22/71-4/12/86	IV	B,U,V	0.12
NRAO 530	17 30 13.4	-13 02 46	50	7/11/72-8/10/85	IV*	PG	0.16
3C 371	18 07 18.3	+69 48 56	150	12/16/68-11/6/85	III	PG	0.12
OX 074	21 44 43.2	+09 15 43	121	5/13/70-11/11/85	III	PG	0.15
BL LAC	22 00 39.0	+42 02 08	306	6/24/71-1/15/85	I	B,U,V,I	0.08
3C 446	22 23 10.5	-05 12 23	154	9/15/71-11/14/85	III	B	0.14
3C 454.3	22 51 29.2	+15 52 54	116	8/20/71-12/13/85	I	B	0.12
2345-16	23 45 27.2	-16 48 11	175	10/10/69-12/3/85	IV	PG	0.13

* INDICATES SUBCLASS CHANGE FROM PAPER I.

AO 0235+164. This is another BL Lac type OVV. A 5 mag outburst (Pica *et al.* 1980b) in 1979 displayed morphology similar to an outburst that occurred in 1975. Further monitoring revealed rapid variations of about 3 mag, but no major flare was seen in 1983 to indicate that the 1975 and 1979 flares were part of a periodic phenomenon. Observations during 1985-1986 failed to image the object on a number of occasions, even though the plates showed stellar images down to magnitude 19.4. Late 1986 and early 1987 observations showed a dramatic 3.2 mag flare, details of which will be published in a subsequent paper.

All pre-1981 data were rereduced for this paper, using an extended comparison sequence that incorporated new comparison stars fainter than 18th magnitude to avoid extrapolation of the faint end of the calibration curve.

OE 110. The paucity of data since 1978 is primarily due to its faintness since that date. Twenty-nine exposures were made between 1978 and 1986, most with plate limits below 19th magnitude. Only nine of these imaged the object. These limited data prevent any comparison of recent variability with pre-1979 activity. Regression analysis shows a linear trend toward a decreasing mean of 0.12 mag per year although the determination is influenced by the patchy sampling after 1980.

PKS 0420-01. This quasar is very active, exhibiting 2 mag outbursts on a timescale of a few years. The activity during 1977 and 1978 seems to be duplicated during the 1982-1983 observing period. The bright point on 20 Novem-

ber 1979 seems to be a real flare, representing an increase of 1.3 mag in five days, followed by a 1.7 mag decrease in 23 days. This observation is based on only one point, but the plate was carefully examined for defects, with negative results.

3C 120. This Seyfert galaxy has been observed regularly at RHO since 1971. The nebulosity around 3C 120 due to the underlying galaxy is visible on plates even with 3 min exposures. To keep the galaxian contribution to the final magnitude constant, all iris measurements since 1981 have been made with a fixed 6 arcsec aperture, which is always large enough to encompass the Airy disk of the nuclear component. All of the pre-1981 data reported here were rereduced using the fixed-iris method. Comparison of the data reduced with both methods revealed differences of nearly 0.4 mag in some cases, but the average difference for 92 observations was only 0.1 mag. The sense of the difference was that the fixed-iris method consistently produced fainter magnitudes than the variable-iris technique.

The long decline in average brightness noted in Paper III between 1971 and 1979 reversed in late 1979, and 3C 120 gradually brightened until mid-1983, subsequent to which another decline appears to have set in. No major flare activity was seen at RHO, although the slow, long-timescale variability seems to have rapid 0.5 mag variations or "flickering" on timescales of weeks.

NRAO 190. This OVV shows increasing variability as we gather more data, and its range now exceeds 4 mag. It has

TABLE III. (continued)

1508+32 B CONT.

Table with 4 columns: U.T. DATE, J.D., MAG., RMS. #. Contains data for 1508+32 B CONT. with various magnitude and RMS values.

1514-24 B CONT.

Table with 4 columns: U.T. DATE, J.D., MAG., RMS. #. Contains data for 1514-24 B CONT. with various magnitude and RMS values.

1514-24 B

Table with 4 columns: U.T. DATE, J.D., MAG., RMS. #. Contains data for 1514-24 B with various magnitude and RMS values.

NR40 512 P CONT.

Table with 4 columns: U.T. DATE, J.D., MAG., RMS. #. Contains data for NR40 512 P CONT. with various magnitude and RMS values.

NR40 512 P

Table with 4 columns: U.T. DATE, J.D., MAG., RMS. #. Contains data for NR40 512 P with various magnitude and RMS values.

3C 345 P CONT.

Table with 4 columns: U.T. DATE, J.D., MAG., RMS. #. Contains data for 3C 345 P CONT. with various magnitude and RMS values.

3C 345 B

Table with 4 columns: U.T. DATE, J.D., MAG., RMS. #. Contains data for 3C 345 B with various magnitude and RMS values.

TABLE III. (continued)

Table with 4 columns: U.T. DATE, J.D., MAG., RMS. #. Contains data for BL LAC V CONT. with 12 rows.

Table with 4 columns: U.T. DATE, J.D., MAG., RMS. #. Contains data for BL LAC I with 27 rows.

Table with 4 columns: U.T. DATE, J.D., MAG., RMS. #. Contains data for SC 446 B with 27 rows.

Table with 4 columns: U.T. DATE, J.D., MAG., RMS. #. Contains data for SC 454.3 B with 47 rows.

Table with 4 columns: U.T. DATE, J.D., MAG., RMS. #. Contains data for SC 446 B CONT. with 27 rows.

Table with 4 columns: U.T. DATE, J.D., MAG., RMS. #. Contains data for SC 454.3 B with 27 rows.

Table with 4 columns: U.T. DATE, J.D., MAG., RMS. #. Contains data for SC 454.3 B with 47 rows.

Table with 4 columns: U.T. DATE, J.D., MAG., RMS. #. Contains data for SC 454.3 B CONT. with 27 rows.

Table with 4 columns: U.T. DATE, J.D., MAG., RMS. #. Contains data for SC 454.3 B with 27 rows.

Table with 4 columns: U.T. DATE, J.D., MAG., RMS. #. Contains data for SC 454.3 B with 47 rows.

Table with 4 columns: U.T. DATE, J.D., MAG., RMS. #. Contains data for SC 454.3 B CONT. with 27 rows.

Table with 4 columns: U.T. DATE, J.D., MAG., RMS. #. Contains data for SC 454.3 B with 27 rows.

Table with 4 columns: U.T. DATE, J.D., MAG., RMS. #. Contains data for SC 454.3 B with 47 rows.

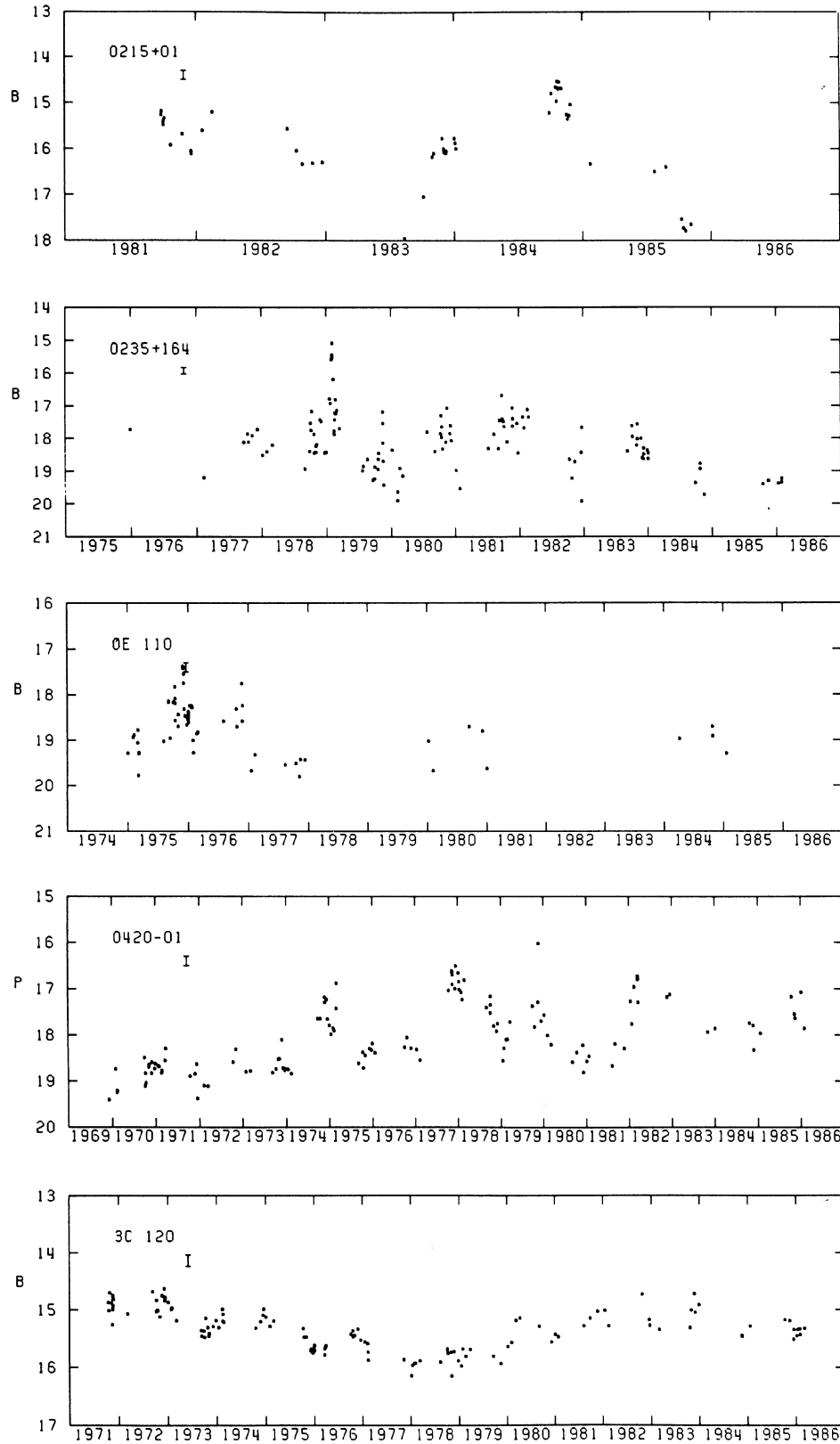


FIG. 1. Light curves of 22 optically violent variable extragalactic sources. The color system used for each graph is denoted on the ordinate. OJ 287 and BL Lac are shown out of right ascension order to conserve space. The error bar under the source name represents 0.2 mag.

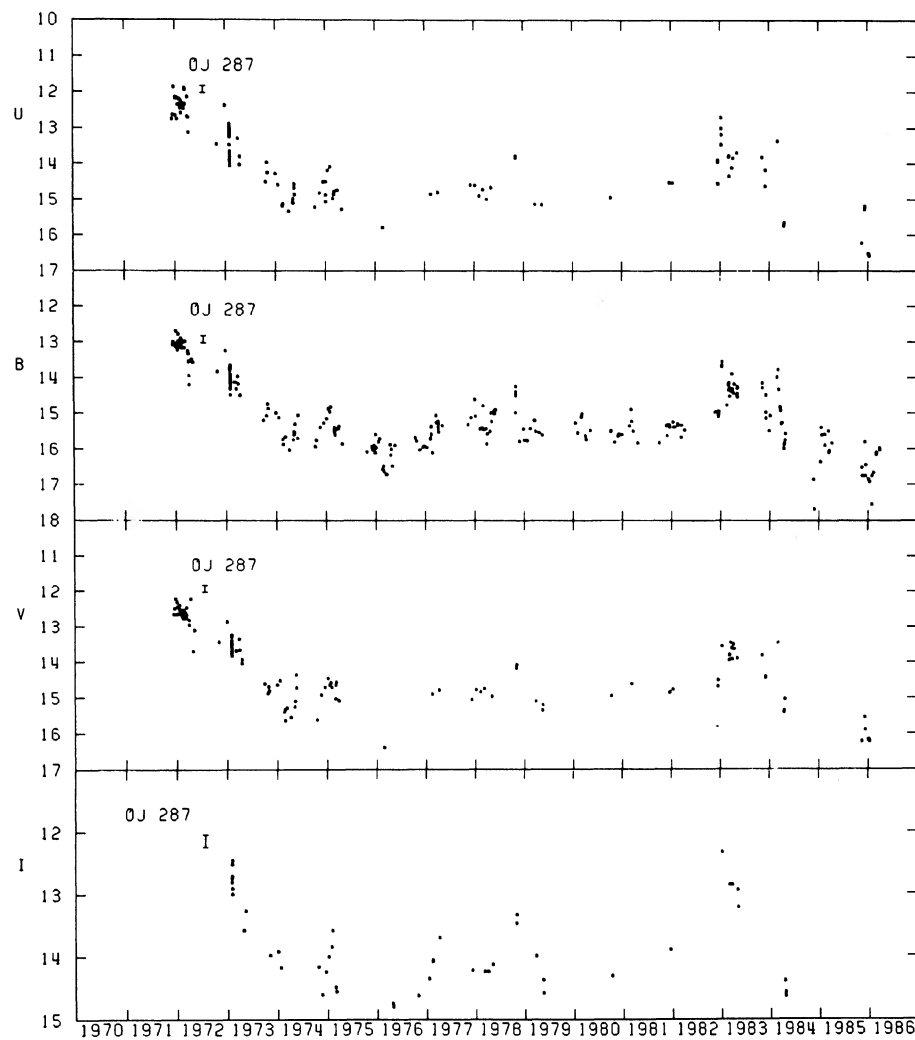
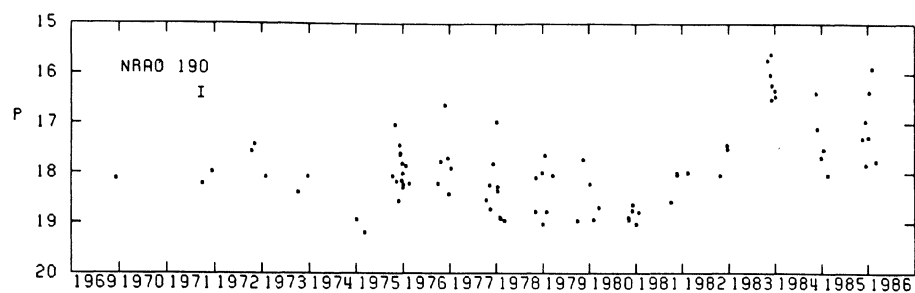


FIG. 1. (continued)

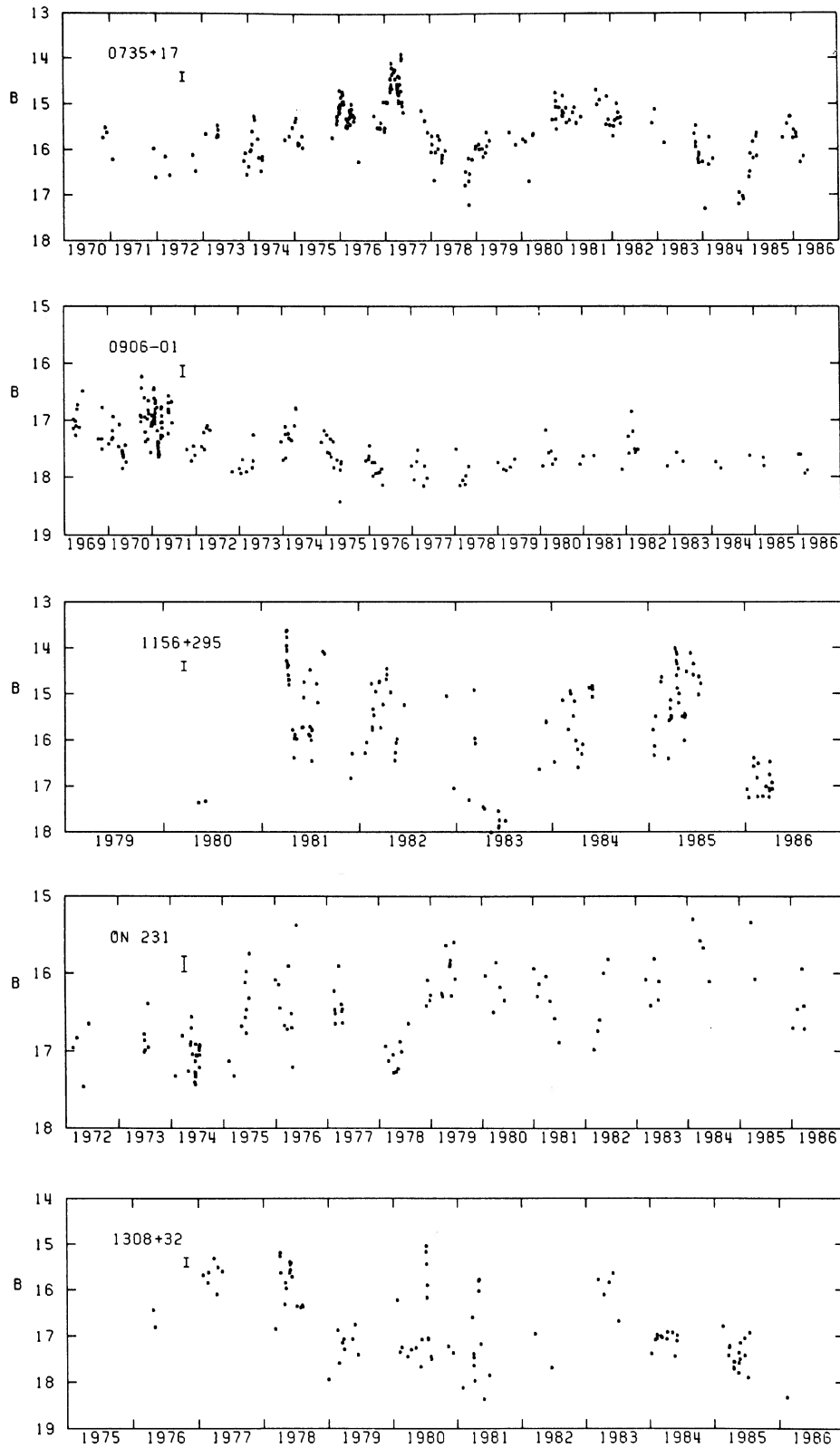


FIG. 1. (continued)

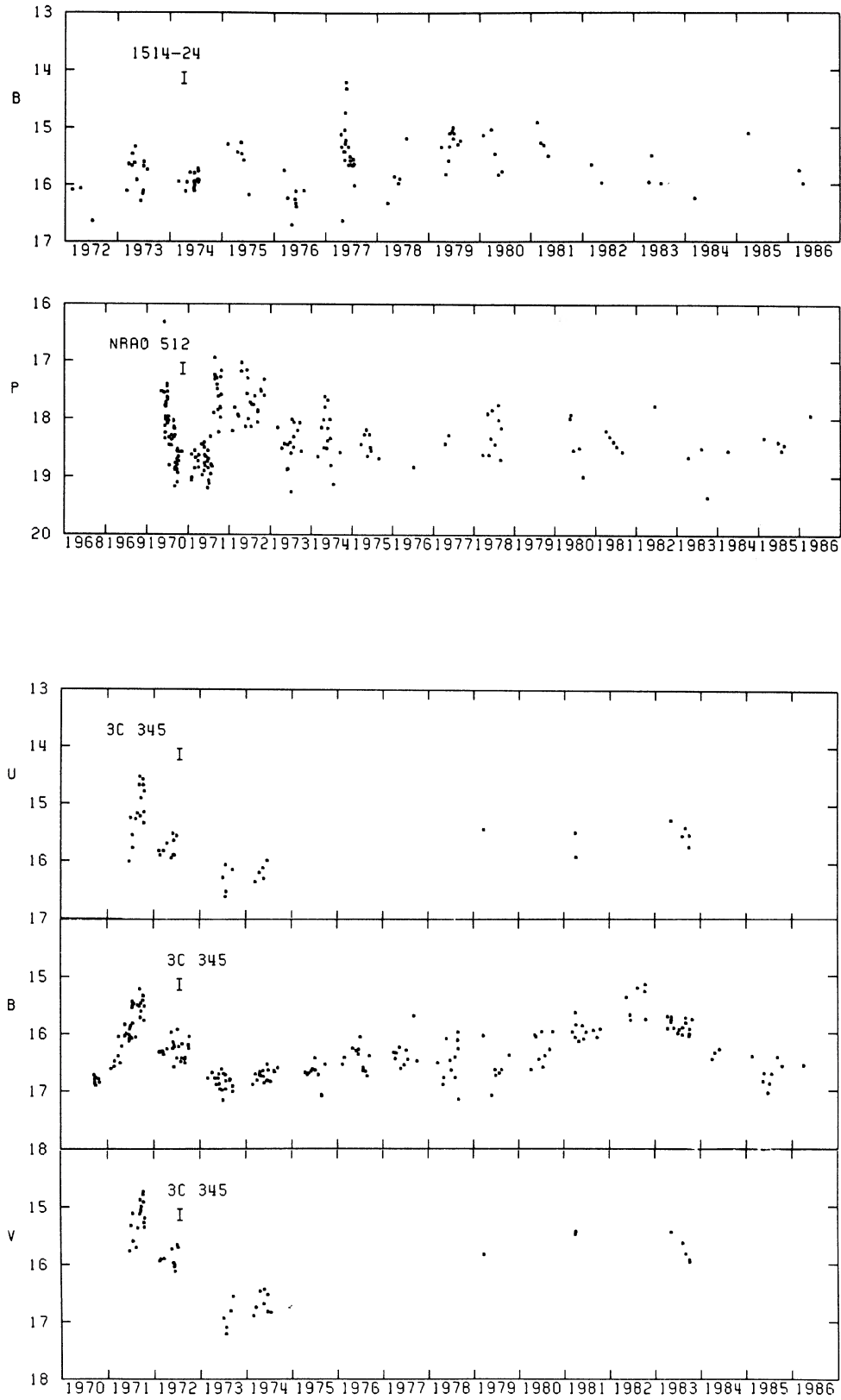


FIG. 1. (continued)

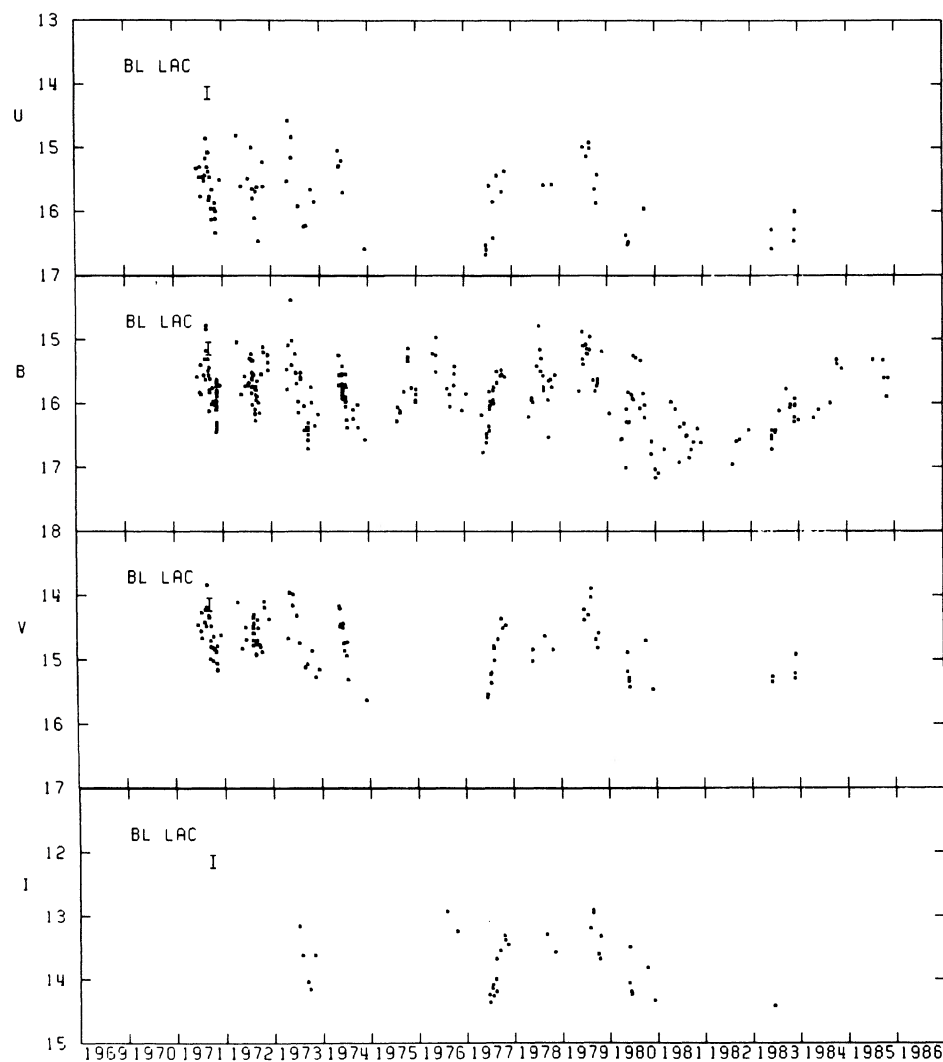
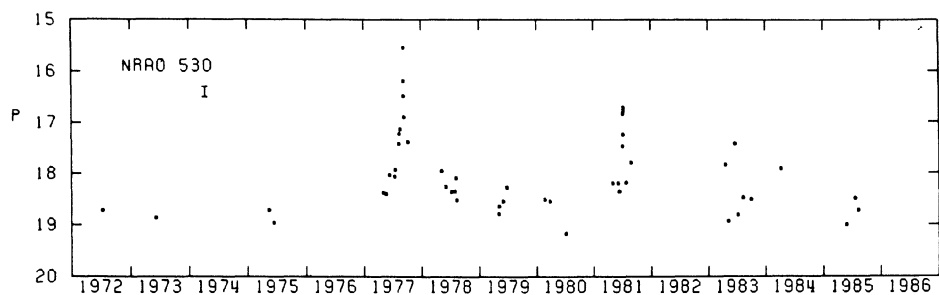


FIG. 1. (continued)

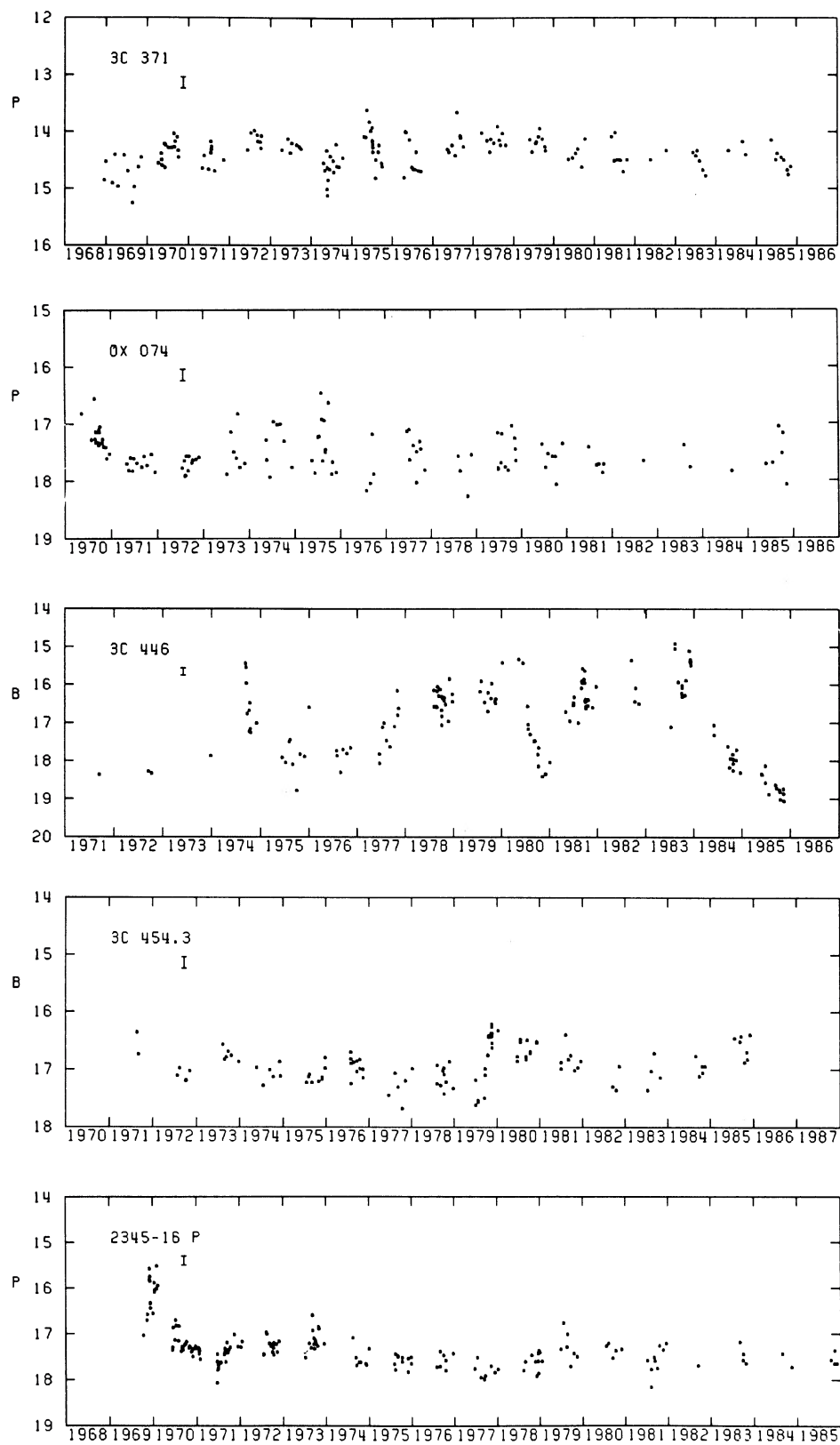


FIG. 1. (continued)

been very active, particularly in recent years, exhibiting an increase of 1.4 mag in 28 days in early 1986. This rapid brightening was followed by a 1.9 mag decrease over a 34 day period. The object was seen as bright as 15.6 on 1 December 1983.

0735 + 17. This highly variable BL Lac has been the subject of many detailed studies. Multifrequency observations including the RHO data were analyzed by Bregman *et al.* (1984). The optical light curve suggests long-term trends with amplitudes of about 2 mag, with more rapid flares of 1–1.5 mag, superimposed.

OJ 287. This active BL Lac object has been heavily monitored at RHO since 1971 and has shown variability over a 5 mag range. The recent outbursts in 1983 and 1984 were followed by a general decline in brightness. Seen at $B = 13.8$ on 9 March 1984, OJ 287 rapidly faded to $B = 16.0$ on 20 April 1984. By late 1984 it had faded to $B = 17.7$, but proceeded to brighten throughout early 1985. A linear-regression analysis indicates a decrease in average brightness of about 0.15 mag per year. The light curve in Fig. 1 contains the early PG data converted to the B system by an empirically determined B -PG correction of $+0.50$.

Analysis of the 1972 and 1983 outbursts by Sillanpää *et al.* (1985) found the morphology of the two outbursts to be very similar. The polarization of OJ 287 during optical outbursts is discussed in Sitko *et al.* (1985).

0906 + 01. After the initial activity seen in 1970–1971, 0906 + 01 has been relatively quiescent. An outburst of 0.8 mag in two months occurred in early 1982. Since that time 0906 + 01 has been inactive. The early PG magnitudes in Table III can be converted to B magnitudes by an offset of B -PG = $+0.20$, based on a series of B and PG exposures taken within minutes of each other on several occasions.

1156 + 295. This quasar is one of the most variable observed. First identified by Wills (1966) as the optical counterpart of the radio source 4C 29.45, it was added to the RHO list in 1980. The 20 star comparison sequence was calibrated by photographic transfer from the ON 231 field. Comparison-star magnitudes and a finder chart for the RHO sequence are published in Wills *et al.* (1983). In early 1981, a 4 mag outburst was detected at RHO. Cooperative observations of this outburst covering the spectrum from radio through ultraviolet are reported by Wills *et al.* (1983) and by Glassgold *et al.* (1983). The extremely erratic variations continued throughout 1984, and in 1985 another outburst, with an amplitude of 2.5 mag, was observed at RHO. Coordinated x-ray and optical observations of this outburst were made with the *EXOSAT* x-ray satellite and the RHO 76 cm telescope. The results of these simultaneous observations are still under analysis, but a preliminary report can be found in Webb and McHardy (1986). Recent optical monitoring shows 1156 + 295 flickering between 16th and 17th magnitude; linear-regression analysis shows decreasing mean brightness at a rate of 0.15 mag per year.

ON 231. This object is another of the BL Lac class. A series of 2 mag outbursts was observed in 1975–1976 and this type of rapid activity has continued through 1986 and early 1987.

1308 + 32. High-amplitude flares and long-term variations characterize the light curve of this BL Lac object. The flares in 1980 and 1981 were closely monitored at RHO, showing an increase in brightness of 2.6 mag between 5 June and 6 July 1980. This increase was followed by a 2 mag decline by 16 July 1980, with another 2 mag flare occurring during April of 1981. This bursting behavior of 1308 + 32

was analyzed by Mufson *et al.* (1985). The linear trend indicates a decrease in mean magnitude of 0.16 mag per year. This object has shown less activity in recent years. Early 1987 observations indicate that 1308 + 32 is at a very faint stage, with $B > 18.8$.

1514 – 24. This BL Lac, also called AP Librae, has been observed at RHO since 1972. One major outburst was seen in 1977. Since that time, little major bursting activity has been detected, although there is evidence of a long-term rise and fall of about a magnitude between 1977 and 1984. A moderate flare in 1985 may have escaped detection because of a paucity of observations. Flickering with an amplitude of a magnitude is common.

NRAO 512. This is another OVV whose initially violent behavior appears to have tapered off. It is possible that some events since 1976 were missed due to apparently sparse sampling, but on many of the plates taken during this interval NRAO 512 was simply below the plate limit. The major flare in 1970 had an amplitude of 3 mag, followed by subsequent events of 1 to 2 mag. Rapid changes of the order of a magnitude are seen in the post-1979 data.

3C 345. This object is one of the most active QSOs, although it fails to display the very rapid bursting behavior seen in sources such as 1308 + 32 and 0235 + 164. Major long-term variations with amplitudes of 2 mag are seen in 1970–1973 and 1980–1985. Short-term flickering is superimposed on the long-term variations with amplitudes of 0.5–1.0 mag. A detailed multifrequency analysis of this source was presented by Bregman *et al.* (1986), who included extensive optical, radio, and ultraviolet data. A correlation between the optical outbursts and the production of superluminally expanding radio sources was reported there. The light curve of 3C 345 has been analyzed a number of times in search of periodic behavior. The work of Smyth and Wolstencroft (1970) and other analyses will be discussed in Sec. IV.

NRAO 530. The recent sampling of this normally faint, bursting QSO is not sufficiently dense to define the bursting activity seen earlier. In spite of the sampling problem, a major outburst was detected in 1981 and another in 1985. These outbursts had amplitudes near 2 mag over periods of weeks.

3C 371. This N type galaxy has been observed to vary over a 2 mag range in the optical region. Optical activity since 1979 has been confined to a 1 mag range between PG = 14.0 and PG = 15.0.

The plates were all re-examined because of our concern over the nebulosity around the stellar nucleus. Exposures made after 1981 were all reduced using a fixed-iris setting to limit and standardize the contribution of the surrounding galaxy. Tests with exposures made before 1981 showed that any systematic errors due to the galaxian component were no larger than the usual rms errors. This is in contrast to the 3C 120 plates, which were completely rereduced because similar tests revealed differences between the fixed and variable-iris methods greater than the normal rms errors. Multifrequency observations of 3C 371 including RHO data were reported by Worrall *et al.* (1984).

OX 074. This QSO showed three large-amplitude events in the interval 1973–1975. Since 1979, only a small outburst in 1985 is prominent in the light curve, although other events could have been missed due to the infrequent observations made between 1982 and 1984.

BL Lac. The prototype of the BL Lacertae class of AGN, this object is well known as one of the most active sources observed. The RHO data show rapid, 1–2 mag flares occur-

ring frequently from 1971 to 1981. Then a slow brightening from $B = 17.2$ on 4 January 1981 to $B = 15.6$ on 15 November 1985 occurred with relatively little flaring activity. This change in the variability characteristic will be closely monitored in the future at RHO.

Photometric data published by Hagen-Thorn *et al.* (1984) agree well with the RHO data when nearly simultaneous observations are compared.

3C 446. This BL Lac type AGN exhibits large, spikelike outbursts and slow, large-amplitude variations. No major spikelike outbursts have been observed since 1974; rather, large-amplitude variations over a number of years seem to dominate the light curve. Observations made in late 1985 showed 3C 446 to be at its all-time faintest measured magnitude, 19.1, but by late 1986 it had gradually recovered to $B = 17.5$. The multifrequency spectral distribution of 3C 446, including the RHO data, has been analyzed by Brown *et al.* (1986), and other multifrequency work is in progress by Bregman (1986).

3C 454.3. This OVV was rather quiescent during the early years of monitoring at RHO, but a fast 1.5 mag flare occurred in late 1979. Following the outburst, the brightness declined slowly for about 3 yr, with flickering similar to that seen before 1979. Since 1983, a general brightening has been observed.

2345–16. The outburst in 1969 is the only major event observed in this QSO. Its behavior since 1970 would not qualify it as an OVV. Rapid, low-amplitude fluctuations of about 0.5 mag are present in the light curve.

IV. ANALYSIS

Many attempts have been made to detect periodicities in QSOs and related objects (Smyth and Wolstencroft 1970; Jurkevich *et al.* 1971). Periodicities on the order of 100–1000 days were reported for 3C 345 by Smyth and Wolstencroft and by Barbieri *et al.* (1977). Evidence for 350 day and 22.5 yr periods in the light curve of 3C 120 was seen by Jurkevich *et al.* Recent periodic analysis of 3C 345 by Babadzhanyants and Belokon (1984) and of 3C 446 by Barbieri *et al.* (1985) detected periodic behavior on the order of thousands of days in both sources.

The nature of optical observations of faint objects makes the detection of periodicities, if any exist, extremely difficult. Unequal intervals of time between observations and annual gaps in the data extending over several months complicate any analysis, along with normal observational uncertainties and the relatively short baselines of the data sets (often only one or two “periods”).

The construction of long-term light curves using data gathered by the same instruments and reduced by the same procedures is ideal for investigating the variability behavior of AGNs. Data collected at RHO extend over 18 yr in some cases. The observing frequency for each object is between two observations per week and a few per year, depending on historical variability characteristics. Generally, for OVVs, the observing frequencies range between one per month and two per week. An object undergoing an outburst is often observed every clear night during its active phase. The reduced sampling frequency in recent years for a few of the objects reported here was in part due to heavy commitments to cooperation with active satellites such as *IUE*, *EXOSAT*, and *IRAS*.

The data were first analyzed for long-term linear trends by

the linear-regression routine given by Bevington (1969). The fit was weighted using instrumental weighting and then removed from the data. The data were then analyzed by the unequal-interval Fourier transform method discussed by Deeming (1975).

Figure 2 shows the power spectra of 3C 120, 3C 345, and 3C 446. The spectral window of 3C 345 is also shown. The spectral window is used to identify aliases that contaminate the power spectrum. Generally, the spectral windows for the data analyzed here show a peak at 1 yr, which represents the annual “observing season” for each object; however, some of the less frequently monitored objects exhibited very complex spectral windows with broad primary and secondary peaks. The features are labeled according to the periods they represent, and possible aliases are labeled in brackets. Only the spectral window of 3C 345 is shown, because it is identical with the spectral windows of the two other sources. The significance of the spectral features in the power spectra of 3C 120, 3C 345, and 3C 446 has been estimated by Monte Carlo simulations. The original magnitudes have been randomly scrambled among the original epochs and then Fourier analyzed. The most prominent spectral features in these simulated spectra were then compared with the original spectral features. The significance of the original spectral peak is defined as

$$s = \frac{P(\text{original})}{\bar{P}(\text{simulated})} \quad (1)$$

$P(\text{original})$ is the power in the original feature and $\bar{P}(\text{simulated})$ is the average power of the strongest peaks seen in the simulated power spectra for a given object. The noise level, $\bar{P}(\text{simulated})$, is shown in Fig. 2 for each power spectrum.

Table IV lists the results of Fourier transform analysis for each of the 22 sources. Column 1 gives the object name, while columns 2–4 list the periods identified with the three most powerful peaks in the power spectrum. Columns 5–7 give the normalized power of each periodic component. Column 8 contains comments about the power spectrum of the source.

Models of the light curves can be constructed based on the periodic components identified by the Fourier analysis (Barbieri *et al.* 1977). The model can be written as

$$m = A + Bt + \sum C_i \cos \left[\frac{2\pi t}{P_i} + \xi_i \right] \quad (2)$$

In Eq. (2), A and B are the intercept and slope given by the regression analysis. The C_i s are the amplitudes for each periodic component. The ξ_i s are the phase shifts in radians, which can be calculated by taking the arctangent of the ratio of the imaginary and real parts of the Fourier transforms.

The model resulting from the Fourier analysis was fitted only to the data for 3C 120, 3C 345 and 3C 446, which were selected because of the extensive data available and the existence of previous timescale analyses in the literature. A fitting scheme that combines the Gauss–Newton and BFGS curve-fitting procedures was used to fit the models to the data. This “hybrid method” (Jacobs 1977) was used to adjust the linear coefficients and the amplitudes and phases of the sinusoidal components to achieve the best possible fit. The starting parameters for the linear coefficients were taken from the regression analyses, while starting values for the cosine parameters were deduced from the Fourier results. The periods were not adjusted by the fitting process and were taken from Table IV. The results are shown in Table V. All

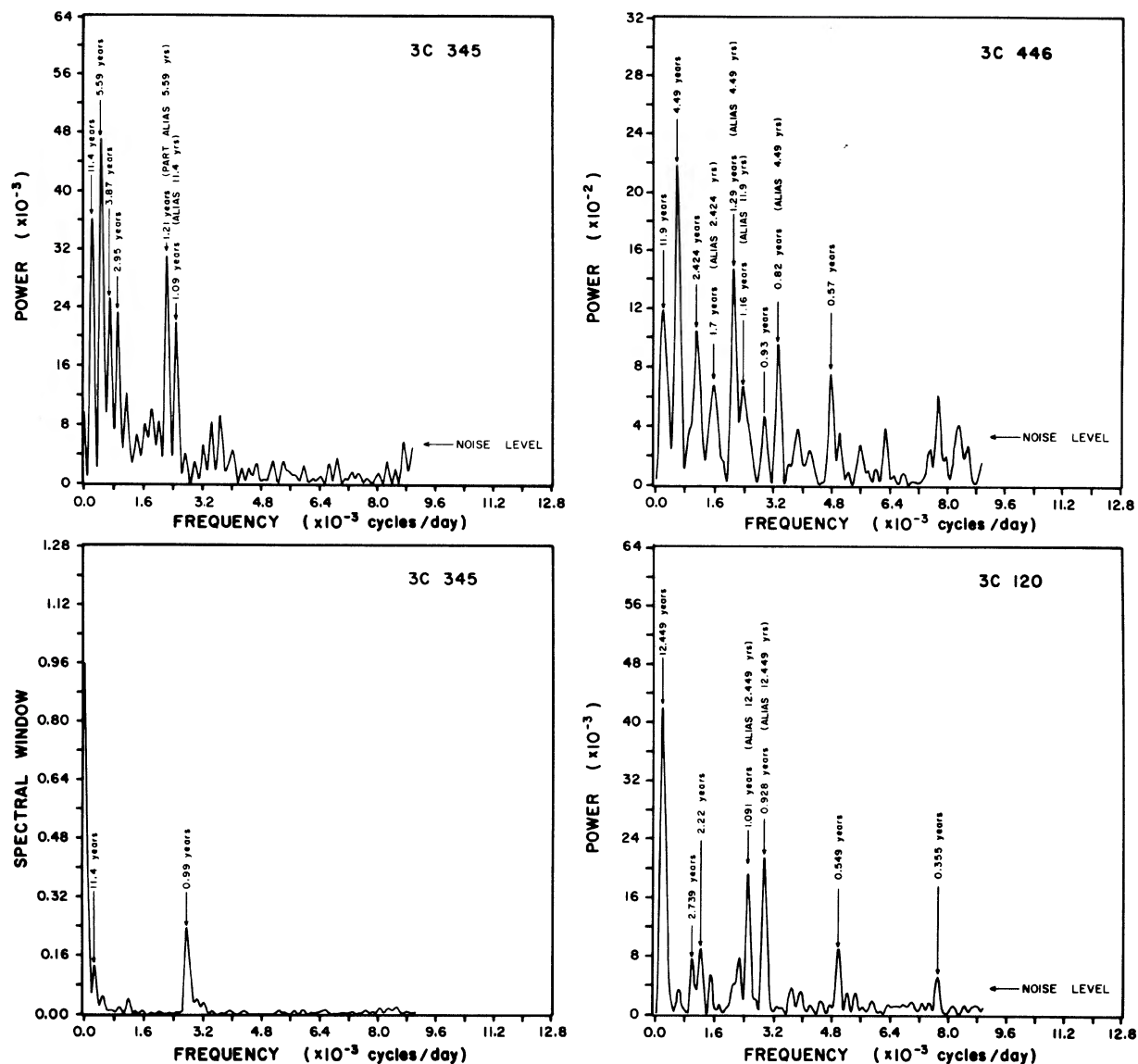


FIG. 2. Power spectra of 3C 120, 3C 345, and 3C 446. The spectral window of 3C 345 is similar to the spectral windows of the other sources. Each major peak is labeled with the corresponding period in years. The brackets associated with some peaks denote that the peak is an alias of the peak given in the brackets. The background-noise level determined by the Monte Carlo calculations is 0.004 for 3C 120, 0.004 for 3C 345, and 0.03 for 3C 446.

though no acceptable fit was found for 3C 466, the best-fit parameters are included in Table V. The 3C 446 data resisted fitting because of extremely rapid, high-amplitude variations whose durations were much less than the resolution of the Fourier analysis. Figure 3 shows the data for 3C 120 and 3C 345 with the fitted curves superimposed. The deviations from the fitted curve represent rapid variations with time-scales smaller than the resolution of the Fourier analysis. As mentioned earlier, the resolution is set by the existence of large gaps in the data, some nearly 5 months long. Even with the scatter due to observational errors and high frequency variations, underlying structure is evident in the light curves of 3C 120 and 3C 345.

3C 120. A periodic analysis of the light variations in 3C 120 using a periodogram technique was reported by Jurke-

vich, Usher, and Shen (1971). Analyzing observations made between 1929 and 1970, they found periods of about 22.5 and 0.96 yr with high-frequency components of $0.05\text{--}0.002\text{ day}^{-1}$.

Fourier analysis of the RHO data yielded only one significant peak in the power spectrum, corresponding to a period of 12.45 yr. The significance of this peak was $s \approx 22$. Although the data run is not sufficiently long to cover more than one cycle, it does reflect the presence of this sinusoidal component. Other peaks were a factor of 10 weaker than the 12.45 yr peak. The 0.96 yr period found by Jurkevich *et al.* is not seen in the power spectrum of the RHO data.

3C 345. A Fourier analysis of the light variations of 3C 345 was presented by Smyth and Wolstencroft (1970). They detected components having periods of 2.8, 1.52, and 0.45 yr

TABLE IV. Fourier transform results.

SOURCE	PERIOD (YRS)			POWER			COMMENTS
	1	2	3	1	2	3	
0215+01	2.17	0.73	----	0.220	0.133	-----	UNDERSAMPLED.
0235+164	2.79	1.53	1.29	0.135	0.096	0.086	
OE 110	2.88	0.29	----	0.049	0.067	-----	UNDERSAMPLED
0420-01	13.04	4.64	2.46	0.042	0.035	0.035	COMPLEX SP. WINDOW.
3C 120	12.45	----	----	0.041	-----	-----	S = 22 1
NRAO 190	3.65	0.88	----	0.044	0.052	-----	
0735+17	4.89	1.20	----	0.153	0.111	-----	#2 POSSIBLY ALIASED.
OJ 287	11.90	5.30	2.79	0.254	0.187	0.059	
0906+01	3.70	2.79	----	0.009	0.009	-----	
1156+295	3.38	1.41	0.52	0.153	0.208	0.090	LIMITED DATA.
ON 231	3.91	1.94	0.78	0.042	0.029	0.033	
1308+32	5.59	1.59	1.28	0.047	0.045	0.025	COMPLEX SP. WINDOW.
1514-24	1.98	0.70	----	0.053	0.026	-----	
NRAO 512	2.46	0.66	----	0.025	0.034	-----	COMPLEX SP. WINDOW.
3C 345	11.40	5.60	----	0.036	0.047	-----	S = 9, S = 11.5 1 2
NRAO 530	4.80	1.71	1.03	0.119	0.140	0.759	UNDERSAMPLED.
3C 371	2.38	0.99	----	0.008	0.007	-----	BLENDED FEATURES.
OX 074	5.07	2.46	0.48	0.007	0.004	0.005	
BL LAC	0.88	0.60	0.31	0.010	0.012	0.022	
3C 446	4.70	2.40	1.29	0.217	0.105	?	S = 7, S = 3, S = ? 1 2 3
3C 454.3	6.39	2.97	0.83	0.011	0.007	0.013	
2345-16	5.07	3.34	1.06	0.028	0.019	0.018	

S = IS THE RELATIVE STRENGTH OF THE FEATURE RELATIVE TO THE NOISE LEVEL AS DETERMINED BY MONTE CARLO SIMULATIONS.

TABLE V. Modeling results.

SOURCE	COEFFICIENT	STANDARD DEVIATION OF COEFFICIENT
MODEL FORM: $M(T) = A + B \cdot T + \sum C_i \cos(2\pi T/P_i + D_i)$		
M = MAGNITUDE IN JOHNSON B BAND.		
A = LINEAR CONSTANT (INTERCEPT IN TABLE 4).		
B = LINEAR COEFFICIENT (SLOPE IN TABLE 4).		
C = AMPLITUDE OF THE COSINE TERM.		
D = PHASE OF THE COSINE TERM.		
P = PERIOD OF THE COSINE TERM (PERIOD IN TABLE 5).		
T = JULIAN DATE MINUS 2,400,000.		
THE COSINE ARGUMENT IS IN RADIANS.		
3C 120	A = 12.99 B = 5.52E-5 C = 0.400 D = 0.30	0.52 1.18E-5 0.024 0.07
3C 345	A = 18.09 B = 4.06E-5 C ₁ = 0.348 D ₁ = -1.25 C ₂ = 0.361 D ₂ = 0.48	0.52 1.19E-5 0.029 0.08 0.275 0.07
3C 446	A = 20.76 B = -8.56E-5 C ₁ = 0.668 D ₁ = 0.14 C ₂ = 0.504 D ₂ = -1.45 C ₃ = 0.183 D ₃ = -0.72	2.19 4.94E-5 0.102 0.18 0.089 0.17 0.088 0.63

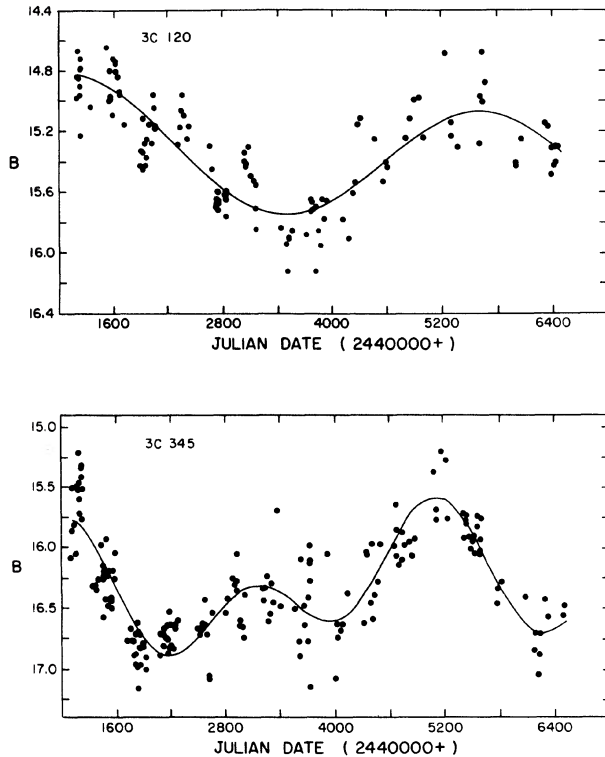


FIG. 3. Light curves of 3C 120 (top) and 3C 345 (bottom) with the fitted model superimposed. The functional form and fitted parameters of each model are listed in Table V. The data points are all *B* magnitudes from Table III.

in observations made between 1965 and 1969. Later work by Barbieri *et al.* (1977) analyzed observations made between 1964 and 1976 using the Deeming-type Fourier analysis. They concluded that the light curve can be characterized by three components with periods of 1600, 800, and 140 days. A more recent analysis was published by Babadzhanyan and Belokon (1984), who constructed a light curve composed of all available observations between 1965 and 1983. They found a systematic increase of the mean brightness of about 0.05 mag per year, a factor of 10 larger than that seen in the RHO data. They resolved the light curve into three periodic components. The first has a period of 15 yr, with an amplitude of 0.8 mag. Component II has a characteristic period of about 1 yr and an amplitude of 1 mag. The third component has a period of 10 days and a range of amplitudes between 0.3 and 1.5 mag, depending on the flare to be modeled. Kidger and Beckman (1986) extended Barbieri's work and found no periodicities were present.

The analysis of the RHO *B* band observations (Table III) yields two components. One has a period of 11.4 yr with $s = 9$, and the model fit requires an amplitude of 0.35 mag. The second component has a period of 5.6 yr with $s = 11.5$, and an amplitude of 0.36 mag. The data are insufficient to model high-frequency fluctuations with periods less than three months. These high-frequency outbursts have amplitudes in excess of 0.6 mag. The curve is a poor fit to the rapid rise of the 1971 outburst, but the fit to the data between 1972 and 1986 appears acceptable (Fig. 3). The 2.8 yr period found by Smyth and Wolstencroft is about half of the shorter

period detected here. Other than this, none of the other previously identified periodicities are derived by our analysis.

The analysis was further extended by adding to the RHO observations historical data covering the years 1965–1973 (Pollock 1982). The overall data set now included 1052 observations from JD 38905.8 to JD 46523.8. Fourier analysis of the complete 21 yr data set yielded periods of 11.4 yr ($s = 2.5$), 2.16 yr ($s = 9$), and 3.9 yr ($s = 12$).

We then divided the 21 yr data set into two segments, a 6 yr segment prior to JD 41087.4 and a 15 yr segment following JD 41087.4. This division was chosen to coincide with the peak of the 1971 outburst so timescales before and after the event could be compared. The power spectrum of the 6 yr segment showed peaks at 4.03 yr ($s = 7.5$) and 1.98 yr ($s = 20$). The spectrum of the 15 yr segment showed peaks at 10.14 yr ($s = 10$), 5.47 yr ($s = 13.7$), and 3.9 yr ($s = 10$).

It can be seen that the only feature common to all three data sets (the 21 yr set, the 15 yr set, and the 6 yr set) is a peak near 4 yr. However, the amplitude and phase of this peak differ in each case. It should be noted that a weak period of about 4 yr ($s = 6$) also appeared in the spectrum of the RHO-only *B* band data; see Fig. 2.

Irregular variable star light curves show seemingly regular variations interrupted by periods of irregular activity. Some isolated segments even show no variability. Although no physical analogy can be made from this comparison, the morphological characteristics of the light curves can be compared if the amplitudes and timescales are properly scaled. The quasar light curves look remarkably similar to the transition periods seen in irregular variable star light curves. This comparison suggests that quasar light curves are still far too brief to be dissected accurately into periodic components.

3C 446. This highly variable BL Lac object exhibits rapid outbursts, dramatic declines, and long-term (4 yr) events over a 5 mag range. Barbieri *et al.* (1985) analyzed the light curve using data from 1965 through 1984. Using the Deeming algorithm to compute the power spectrum, they found strong peaks corresponding to periods of 4.22 and 5.83 yr. Many of their data points between 1971 and 1978 were observations from RHO, so we analyzed the same data using our Fourier transform program and confirmed their results. Then, Fourier analysis of the more extensive data reported here resulted in the identification of three periods; two are relatively strong and one is blended with an alias. These peaks in the power spectrum occur at 4.7 yr ($s = 7$), 2.4 yr ($s = 3$), and 1.29 yr. The significance of the 1.29 yr period cannot be obtained with any confidence because of the superimposed alias. The period of 4.7 yr is close to the period found by Barbieri and his co-workers, but there is no sign of the 5.83 yr period in our spectra.

If the periodic components identified in the power spectra of the foregoing light curves are manifestations of some periodic physical process, how can these processes be incorporated into current physical models? If the components represent true physical timescales in the object, we cannot use relativistic expansion to circumvent the $r \ll cP$ relationship, where P is the shortest observed timescale (Elliott and Shapiro 1974). In the quasar rest frames, the periods are shorter by a factor of $(1+z)$. For 3C 345, with a redshift of $z = 0.595$, the periods from Table IV are 7.1 and 3.38 yr in the quasar rest frame. 3C 120 has a redshift of 0.032, and the period in the rest frame is 12.06 yr. The periods in the rest frame of 3C 446 are reduced even more due to its large redshift. A redshift of 1.404 reduces the observed periods to

1.95, 1.0, and 0.54 yr, respectively. The periods identified in this work place no severe constraints on emission models via the $R < cP$ relationship. The rapid flares seen in 3C 446 place much tighter constraints on possible models.

One of the first models proposed to explain periodic behavior in quasars was the massive-rotator model (Morrison 1969). This model is a scaled-up version of the pulsar model, characterized by a massive ($\mathcal{M} = 1 \times 10^5 \mathcal{M}_\odot$) collapsed object with a strong magnetic field rotating with a period of about 1×10^7 s. Detailed analyses of magnetodynamic models have been performed by Ozernoi (1966), and Ozernoi and Chertoprud (1967, 1970). They suggest that the slow (cyclic) and rapid (fluctuating) components seen in quasar light curves can be explained in terms of a supermassive, rotating magnetoid. It is not clear how these rotating magnetoids can explain the existence of several cyclic components (such as those seen in 3C 446).

The current generic theory of AGN emission involves massive black holes and accretion disks. Thin-disk structure has been explored in detail (Shakura and Sunyaev 1973 and Novikov and Thorne 1973). These disks parametrize the viscosity in the form of a constant α and are hereafter referred to as alpha disks. In discussing alpha disks, we can calculate various characteristic timescales (Pringle 1981; Sitko 1986) for a particular disk. The basic disk timescale is related to the rotational angular velocity. Sitko (1986) calculates this timescale for a massive disk surrounding a $1 \times 10^8 \mathcal{M}_\odot$ black hole with an accretion rate of $0.1 \mathcal{M}_\odot$ per year. He finds that the rotational timescales for regions of the disk hot enough to contribute substantial flux in the optical band are on the order of hours to several days. This timescale is too short to account for the variations discussed here, even changing the masses and accretion rates over the limited ranges suggested by some observations.

Hydrostatic equilibrium in the z direction is established on the timescale t_z , which is nearly equal to the rotational timescale and thus not applicable here. The thermal timescale is the time it takes the disk material to establish thermal equilibrium if the rate of dissipation is changed. For disk radii of interest here (i.e., those radii where the temperature is high enough to radiate copiously in the optical region), the thermal timescale falls in the required range of days to several years, depending on the value of the viscosity parameter α . The final timescale is the viscous timescale, or the time needed for substantial change in the surface density of the disk. The viscous timescale of an alpha disk is of the order of several months to several years, for reasonable values of alpha. The viscosity controls the accretion rate and thus may be responsible for outbursts, and possibly the "periodic" variations identified in the RHO data. It is interesting to note that models utilizing the thermal and viscous timescales have been used to describe dwarf nova outbursts (Fran, King, and Raine 1986).

Vila (1979) analyzed pulsations perpendicular to the symmetry plane in self-gravitating accretion disks. He notes that the disk pulsates with different frequencies at different radii, so the model is capable of explaining multiple periodic components and he derives the following relationship between the period P of the light variation, the radius R across the disk at which the pulsations occur, and the mass \mathcal{M} of the central hole:

$$PR^{-3/2}\mathcal{M}^{1/2} = 0.035. \quad (3)$$

In Eq. (3), the mass is in grams and the radius is in centi-

meters. Pollock (1982) examined a number of outbursts of 3C 345 and 3C 446. The most rapid significant variation places limits on the size of the central object (presumably a black hole) through the $R < ct$ criterion. Since the emitted energy has to come from a volume with radius less than R , but greater than the Schwarzschild radius, Pollock was able to establish limits on the mass of the central object. Using the mass limits derived by Pollock, we can calculate the radii at which the pulsations occur. The radii calculated by Eq. (3) for reasonable values of the mass of the central black hole, and for the timescales found in the Fourier analyses of 3C 120, 3C 345, and 3C 446, are all about $1-4 \times 10^{17}$ cm. Again, this region of the disk contributes little to the flux in the optical band, so the oscillations would not be seen as the large-amplitude optical components derived here from the RHO data.

V. CONCLUSIONS

We have presented optical data for 22 OVV active galactic nuclei in both graphical and tabular form. These data resulted from over 18 yr of photographic monitoring of more than 200 variable extragalactic sources. Each OVV is assigned a variability subclass depending on the characteristics of its optical light curve. The data are then analyzed for linear trends by least squares. After the linear component is removed from the data, a Deeming-type Fourier analysis is used to investigate the possibility of periodic components in the light curves. The results of this analysis are given in tabular form for all 22 sources. Since several previous publications have identified periodic components in 3C 120, 3C 345, and 3C 446, these objects are discussed in detail, and models incorporating both linear and sinusoidal components are generated. The 3C 120 and 3C 345 curves fit the data well, but the 3C 446 model is not a good representation of the data. The poorer fit is primarily due to rapid, high-amplitude flares in the light curve of 3C 446. The sinusoidal component found for 3C 120 with a period of 12.45 yr, and the components for 3C 345 with periods of 11.4 and 5.6 yr, did not agree with any periodic components suggested by other authors. The previously reported period of 4.2 yr for 3C 446 is close to the 4.7 yr period found here. Two other periods, 2.4 and 1.29 yr, are present in the power spectrum of 3C 446.

The identification of periodic components in a finite data set does not prove the existence of "real" periods in the source caused by periodic physical processes. If the periodic components identified in the data persist in the future, then the theories must account for the quasiperiodic behavior of the light variations. The periodic components identified in a particular segment of the light curve could die out or be replaced by new components. Periodic analysis of later segments might reveal only the new components. This behavior is suggested by the fact that previous analyses found different periods using earlier data. The persistence of the 4.0 yr period in 3C 345 and the 4.7 yr period in 3C 446, while other periods died out and were replaced, might indicate a transition period. Monitoring programs, such as the one at RHO, can provide important evidence as to the nature of the optical activity by continuing to collect variability data on these sources.

Timescales related to accretion models are discussed and compared with the periods found here. The rotational and z timescales in the regions of the disk where the optical emissions originate are too short to account for the observed peri-

odic components. The thermal and viscous timescales are of the right order of magnitude, and variations on these timescales should be investigated.

Pulsations in accretion disks may provide a mechanism to account for periodic behavior in the case of thin disks, but at the radii at which these variations occur the disks are too cool to contribute substantial flux unless unusually hot clumps of material form.

The authors acknowledge Kojo Sonada for rereducing a

large portion of the 3C 120 exposures; as always, a great debt is owed to the many observers who contributed their efforts over the years. J.R.W. would like to thank Dr. Geza Kovacs for several helpful discussions concerning Fourier transform techniques, and Drs. J. H. Hunter and R. Buchler for suggestions concerning this work. All of the work reported here has been made possible by a series of continuing grants from the National Science Foundation, of which the current grant is AST-8516269. We are indeed grateful for this long-term support.

REFERENCES

- Angione, R. J. (1971). *Astron. J.* **76**, 25.
- Babadzhanyants, M. K., and Beloken, E. T. (1984). *Astrofizika* **21**, 231.
- Barbieri, C., Cristiani, S., Omizzolo, S., and Pomano, G. (1985). *Astron. Astrophys.* **142**, 316.
- Barbieri, C., Romano, G., di Serigio, S., and Zambon, M. (1977). *Astron. Astrophys.* **59**, 419.
- Bevington, P. R. (1969). *Data Reduction and Error Analysis for the Physical Sciences* (McGraw-Hill, New York).
- Blades, J. C., Hunstead, R. W., Murdoch, H. S., and Pettini, M. (1982). *Mon. Not. R. Astron. Soc.* **200**, 1091.
- Bolton, J. G., and Wall, J. V. (1970). *Aust. J. Phys.* **23**, 789.
- Bregman, J. N., Glassgold, A. E., Huggins, P. J., Aller, H. D., Aller, M. F., Hodge, P. E., Rieke, G. H., Lebofsky, M. J., Pollock, J. T., Pica, A. J., Leacock, R. J., Smith, A. G., Webb, J. R., Balonek, T. J., Dent, W. A., O'Dea, C. P., Ku, W. H.-M., Schwartz, D. A., Miller, J. S., Rudy, R. J., and LeVan, P. D. (1984). *Astrophys. J.* **276**, 454.
- Bregman, J. N., Glassgold, A. E., Huggins, P. J., Neugebauer, G., Soifer, B. T., Matthews, K., Elias, J., Webb, J. R., Pollock, J. T., Pica, A. J., Leacock, R. J., Smith, A. G., Aller, H. D., Aller, M. F., Hodge, P. E., Dent, W. A., Balonek, T. J., Barvainis, R. E., Roellig, T. P. L., Wisniewski, W. Z., Rieke, G. H., Lebofsky, M. J., Wills, B. J., Wills, F. C., Ku, W. H.-M., Bregman, J. D., Witteborn, F. C., Lester, D. F., Impey, C. D., and Hackwell, J. A. (1986). *Astrophys. J.* (submitted).
- Brown, L. M. J., Robson, E. I., Gear, W. K., Crosthwaite, R. P., McHardy, I. M., Hanson, C. G., Geldzahler, B. J., and Webb, J. R. (1986). *Mon. Not. R. Astron. Soc.* **219**, 671.
- Deeming, T. J. (1975). *Astrophys. Space Sci.* **36**, 137.
- Dent, W. A., Kapitzky, J. E., and Kojoian, G. (1974). *Astron. J.* **79**, 1232.
- Difley, J. A. (1968). *Astron. J.* **73**, 762.
- Elliott, J. L., and Shapiro, S. L. (1974). *Astrophys. J. Lett.* **192**, L3.
- Frank, J., King, A. R., and Raine, D. J. (1985). *Accretion Power in Astrophysics* (Cambridge University, Cambridge).
- Glassgold, A. E., Bregman, J. N., Huggins, P. J., Kinney, A. L., Pica, A. J., Pollock, J. T., Leacock, R. J., Smith, A. G., Webb, J. R., Wisniewski, W. Z., Jeske, N., Spinrad, H., Henry, R. B. C., Miller, J. S., Impey, C., Neugebauer, G., Aller, M. F., Aller, H. D., Hodge, P. E., Balonek, T. J., Dent, W. A., and O'Dea, C. P. (1983). *Astrophys. J.* **274**, 101.
- Hackney, R. L. (1972). Ph.D. dissertation, University of Florida.
- Hagen-Thorn, V. A., Marchenko, S. G., and Yakovleva, V. A. (1984). *Sov. Astron.* **28**, 538.
- Jacobs, D. A., editor (1977). *The State of the Art in Numerical Analysis* (Academic, New York).
- Jurkevich, I., Usher, P. D., and Shen, B. S. P. (1971). *Astrophys. Space Sci.* **10**, 402.
- Kidger, M. R., and Beckman, J. B. (1986). *Astron. Astrophys.* **154**, 288.
- Kinman, T. D. (1978). In *Pittsburgh Conference on BL Lac Objects*, edited by W. M. Wolfe (University of Pittsburgh, Pittsburgh).
- McGimsey, B. Q., Smith, A. G., Scott, R. L., Leacock, R. J., Edwards, P. L., and Hackney, K. R. (1975). *Astron. J.* **80**, 895.
- Mufson, S. L., Stein, W. A., Wisniewski, W. Z., Pollock, J. T., Aller, H. D., and Aller, M. F. (1985). *Astrophys. J.* **288**, 718.
- Morrison, P. (1969). *Astrophys. J. Lett.* **157**, L73.
- Novikov, I. D., and Thorne, K. S. (1973). In *Black Holes*, edited by C. DeWitt and B. DeWitt (Gordon and Breach, New York).
- Ozernoi, L. M. (1966). *Sov. Astron.-AJ* **10**, 241.
- Ozernoi, L. M., and Chertoprud, V. E. (1967). *Sov. Astron.-AJ* **11**, 428.
- Ozernoi, L. M., and Chertoprud, V. E. (1970). *Sov. Astron.-AJ* **13**, 738.
- Penston, M. J., and Cannon, R. (1970). *R. Obs. Bull.* No. 159.
- Pica, A. J., Pollock, J. T., Smith, A. G., Leacock, R. J., Edwards, P. L., and Scott, R. L. (1980a). *Astron. J.* **85**, 1442.
- Pica, A. J., Smith, A. G., and Pollock, J. T. (1980b). *Astrophys. J.* **236**, 84.
- Pica, A. J., Webb, J. R., Smith, A. G., Leacock, R. J., and Bitran, M. (1987). *Astron. J.* **94**, 287.
- Pollock, J. T. (1982). Ph. D. dissertation, University of Florida.
- Pollock, J. T., Pica, A. J., Smith, A. G., Leacock, R. J., Edwards, P. L., and Scott, R. L. (1979). *Astron. J.* **84**, 1658.
- Pringle, J. E. (1981). *Annu. Rev. Astron. Astrophys.* **19**, 137.
- Racine, R. (1970). *Astrophys. J. Lett.* **159**, L99.
- Schoening, W. E. (1977). *Am. Astron. Soc. Photo-Bull.* **14**, 3.
- Scott, R. L., Leacock, R. J., McGimsey, B. Q., Smith, A. G., Edwards, P. L., Hackney, K. R., and Hackney, R. L. (1976). *Astron. J.* **81**, 7.
- Scott, R. L., and Smith, A. G. (1976). *Am. Astron. Soc. Photo-Bull.* **12**, 6.
- Scott, R. L., Smith, A. G., and Leacock, R. J. (1977). *Am. Astron. Soc. Photo-Bull.* **15**, 12.
- Shakura, N. I., and Sunyaev, R. A. (1973). *Astron. Astrophys.* **24**, 337.
- Sillanpää, A., Teerikorpi, P., Haarala, S., Korhonen, T., Efinov, Y. S., and Shakhovaskay, N. M. (1985). *Astron. Astrophys.* **147**, 67.
- Sitko, M. L. (1986). In *Proceedings of the Workshop on Continuum Emission of AGNs*, edited by M. Sitko (NOAO, Tucson).
- Sitko, M. L., Schmidt, G. D., and Stein, W. A. (1985). *Astrophys. J. Suppl.* **59**, 323.
- Smyth, M. J., and Wolstencroft, R. D. (1970). *Astrophys. Space Sci.* **8**, 471.
- Vila, S. C. (1979). *Astrophys. J.* **234**, 646.
- Webb, J. R., and McHardy, I. (1985). In *Proceedings of the Workshop on Continuum Emission of AGNs*, edited by M. Sitko (NOAO, Tucson).
- Wills, B. J., Pollock, J. T., Aller, H. D., Aller, M. F., Balonek, T. J., Barvainis, R. E., Binzel, R. P., Chaffee, J. R. F. H., Dent, W. A., Douglas, J. N., Fanti, C., Garrett, D. B., Gregorini, L., Henry, R. B. C., Hill, R. E., Howard, R., Jeske, N., Kepler, S. O., Leacock, R. J., Mantovani, F., O'Dea, C. P., Padrielli, L., Perley, P., Pica, A. J., Puschell, J. J., Sanduleak, N., Shields, G. A., Smith, A. G., Thuan, T. X., Wade, C. M., Wasilewski, A. J., Webb, J. R., Wills, D., and Wisniewski, W. Z. (1983). *Astrophys. J.* **274**, 62.
- Worrall, D. M., Puschell, J. J., Bruhweiler, F. C., Miller, H. R., Rudy, R. J., Ku, W. H.-M., Aller, M. F., Aller, H. D., Hodge, P. E., Matthews, K., Neugebauer, G., Soifer, B. T., Webb, J. R., Pica, A. J., Pollock, J. T., Smith, A. G., and Leacock, R. J. (1984). *Astrophys. J.* **278**, 521.